We are IntechOpen,
the world's leading publisher of
Open Access books
Built by scientists, for scientists

4,800

Open access books available

122,000

International authors and editors

135M

Downloads

154

Countries delivered to

Our authors are among the

TOP 1%

most cited scientists

12.2%

Contributors from top 500 universities

CLARIVATE ANALYTICS

BOOK
CITATION
INDEX

INDEXED

WEB OF SCIENCE™

Selection of our books indexed in the Book Citation Index
in Web of Science™ Core Collection (BKCI)

Interested in publishing with us?
Contact book.department@intechopen.com

Numbers displayed above are based on latest data collected.
For more information visit www.intechopen.com

Robust Fiber-Integrated High-Q Microsphere for Practical Sensing Applications

Ying-Zhan Yan[1,2], Shu-Bin Yan[1], Zhe Ji[3], Da-Gong Jia[3], Chen-Yang Xue[2],
Jun Liu[1], Wen-Dong Zhang[1,2] and Ji-Jun Xiong[1,2]
*[1]Key Laboratory of Instrumentation Science and Dynamic Measurement
(North University of China), Ministry of Education, Taiyuan,
[2]Science and Technology on Electronic Test and Measurement
Laboratory, North University of China, Taiyuan,
[3]Key Laboratory of Opto-Electronics Information and
Technical Science, Tianjin University, Tianjin
P. R. China*

1. Introduction

Whispering gallery modes (WGM) resonators (K. J. Vahala, 2003; A. B. Matsko et al., 2006) have been extensively studied in a large variety of geometrical shapes and in a wide range of promising studies and applications (A. Chiasera et al., 2010), both fundamental like *CQED* and practical like low threshold lasers and sensors. The Silica spherical microresonators, made from commercial optical fibers, could support WGM with ultra-high quality factors (Q) (about $10^{7\sim9}$). With the merits of very small model volume and good compatibility with fiber-integrated optics, they are promising for a number of passive and active devices as filters, lasers and modulators (A. Chiasera et al., 2010). In WGMs, the electromagnetic wave is strongly confined within the microcavity in the manner of "totally internally reflection" (TIR). Thus, there is minimal reflection optical losses at the cavity interface. With the negligible silica absorption loss, the resonant modes can reach the ultra-high Q. Benefitting from the high-Q (M. L. Gorodetsky et al., 1996), the WGMs behave as extreme-narrow linewidth resonant dips. Therefore, a small shift of the resonant dip can be detected with high resolution, meaning that the WGMs are potential in the sensing researches (F. Vollmer et al., 2008; Y. Sun et al., 2008; M. Sumetsk et al., 2007; F. Xu et al., 2008; I. M. White et al., 2008). Intuitively (as shown in Fig. 1), photons can travel around many trips inside the high-Q microcavity, and interact with the detected matters around the microcavity many times (Fig. 1-a). By contrast, in the traditional fiber sensors each photon can interact with the detected matters only once (Fig. 1-b). Therefore, the microcavity-based sensors can have more superior performance than the conventional fiber sensors, demonstrating a higher sensitivity or resolution.

However, despite the promising prospect, there are great challenges in the practical microcavity-based sensing devices. The microsphere needs an external fiber taper to excite its WGMs by an external fiber taper (M. Cai et al., 2000). This discrete coupling system can't provide sufficient stability, because the effective coupling can be affected, and even be broken when loading the vibration on the taper or the microsphere. Moreover, the exposure of the
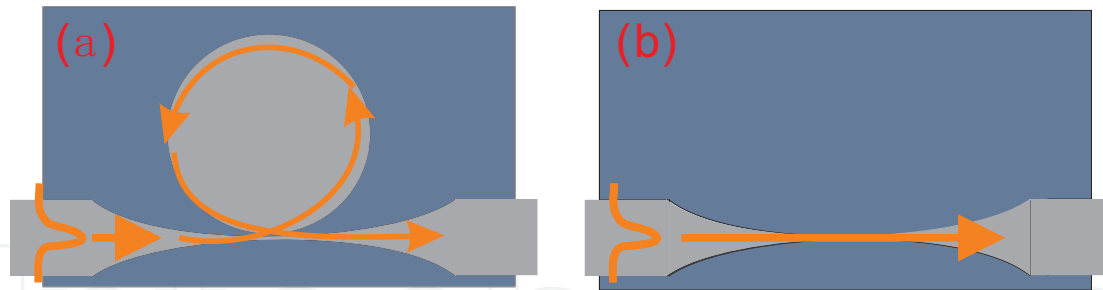
Fig. 1. Comparison of the sensing mechanisms of the microcavity-based sensors and the traditional fiber sensors. (a) The sensing mechanism for the microcavity-based sensor, while (b) for the traditional fiber sensors.

coupling system also makes the Q-maintenance challenging greatly, because the water and the dust in the air could spoil the Q drastically. These above problems are some challenges when promoting the sensing research into practical applications.

In this chapter, we propose one solution to these problems so as to construct a robust structure. Furthermore, we demonstrate the practical thermal sensing application based on the robust fiber-integrated microsphere coupling structure. The flow of this chapter is as follows: First, we introduce the construction of the traditional microcsphere coupling system, and point out the problems which hinder the practical application in the traditional microcavity sensing systems. Then we illustrate the solution to these problems, which for the first time, is proposed by our group. Afterwards, by using our improved robust structure, thermal sensing experiments will be demonstrated to illustrate the practical application. The last section of this chapter is the conclusions and the expectations.

2. Fiber-taper coupled microsphere system

2.1 Fabrication

The excitation of the microsphere WGMs needs an external coupler. Here, the optical tapered fiber is used to excite the microsphere optical modes evanescently. Tapered fibers are first suggested in applications as bidirectional fiber couplers and polarizers in the early 1980s. Mode field evolution in a tapered fiber has been thoroughly studied since then. In order to fulfill a high coupling efficiency between the two parts, phase matching is required where the propagation constant of the fiber taper should be matched to that of the microsphere cavity (J. C. Knight et al., 1997). Consequently, microspheres with different diameters (D) require the tapered fibers with different taper region and different taper angle. To fabricate tapers meeting various demands, a versatile fabrication method is used. Fig. 2-a is the tapered fiber fabrication setup for the heat-drawing manner used in our lab. Firstly, a section of a standard single mode fiber is prepared by removing the plastic coating and then cleaning it with anhydrous alcohol. After that, clamp it on a pair of motorized flats which should be paralleled, and each with a synchronous tunable speed. The thermal resource is a hydrogen microtorch placing underneath the optical fiber prepared. A microscope is installed vertically for monitoring the pulling process. During the procedure, the microtorch is lighted while the two flats move apart in opposite directions at a certain drawing speed. Low loss is essential in this process, and the taper loss is monitored by detecting the power transmission through the tapered fiber with a New-Focus dynamometer. As shown in the insets of Fig. 2-b, a low loss of 2.9 db is achieved through adjusting the two stages to keep them horizontal. This is
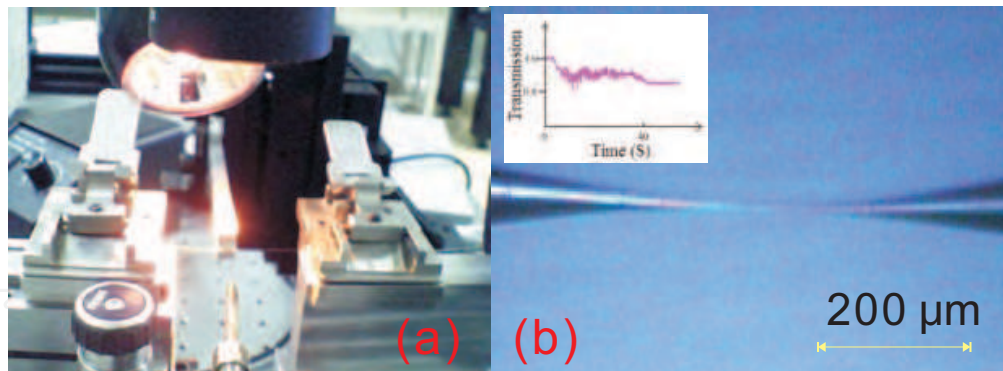
Fig. 2. (a) Tapered fiber fabrication setup in our lab. (b) Typical micrography of a taper, insets: transmission power monitoring during taper fabrication.

the critical point to fabricate the tapered fiber. In addition, the flame position, hydrogen flow and the pulling speed are crucial factors. Through controlling and adjusting these parameters precisely, tapered fibers with desired tapered waist diameter, taper region and taper angle can be prepared, as shown in Fig. 2-b.
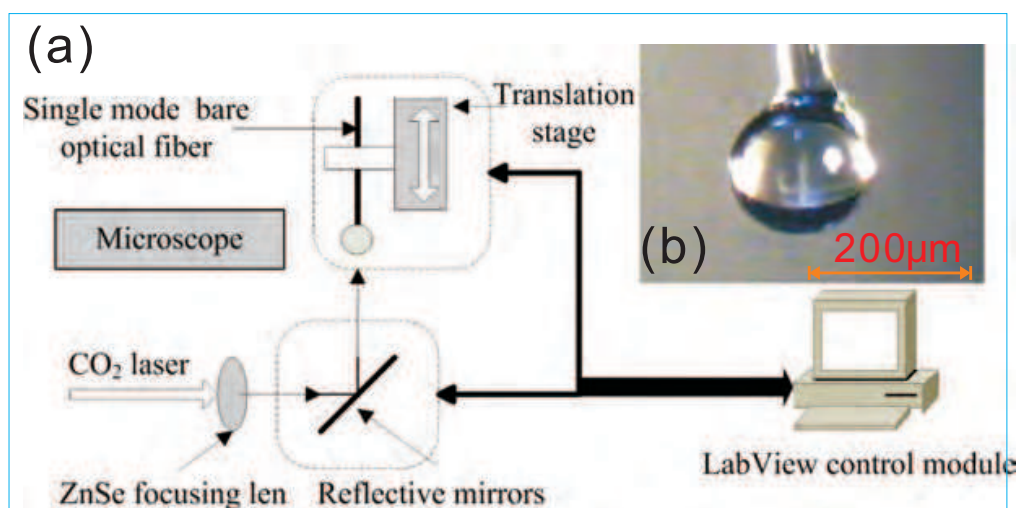

Fig. 3. (a) The schematic plan of the microsphere fabrication setup in our lab. (b) A typical microsphere fabricated in our lab.

Microsphere cavities are made of fused silica due to its ultralow attenuation in the 1550 nm band. This also makes the microsphere compatible with the fiber optical systems. The fabrication procedure is as follows. First, remove the plastic coating of a piece of a silica single mode optical fiber. Then by using tapered fiber fabrication system, heat and pull it into a slender thread taper. Fixing the fiber thread on a high-resolution stage, by controlling the CO_2 laser position, a microsphere grows automatically due to the surface tension. According to the volume conservation, we can control the size of the microsphere by controlling the heating length. The residual fiber attaching to the sphere can help us handle the microcavity conveniently. Fig. 3-a is a schematic plan of the fabrication setup in our lab, in which the coherent CO_2 laser (10.6μm in wavelength) is used as the heating source, due to the strong absorption of silica in the infrared band. The heating laser is guided by reflective mirrors. It is then focused towards the control stages where microspheres are made. A $450 \sim 570X$ microscope is placed vertically to monitor the procedure by using a CCD camera. Other

heating sources, such as the hydrogen flame is also used by several other groups. However, hydrogen flame heating can lead-in hydroxide ion which can induced extra optical loss in the 1550 nm band.

2.2 Resonant characteristic testing

Fig. 4-a shows the schematic plan of the microsphere testing system. Narrow linewidth ($< 300KHZ$), external-cavity New Focus Velocity Laser at the telecommunications band ($1520\ nm \sim 1570\ nm$) is used to pump the microsphere WGMs. Using a polarization controller, the polarization state is controlled to research the influence on the resonance. High efficient coupling between the tapered fiber and the microsphere is obtained through precisely controlling their gap by using a piezoelectric translation stage. Dual microscopes are used to simultaneously monitor the coupling system, horizontally and vertically, respectively. The output signal is collected by the photoreceptor and displayed on the digital oscillograph. Signal-generator generating a triangular wave with frequency $500HZ$ with the peak value less than $3V$ is used to modulate the laser scanning with a modulation width $30GHZ$. Selecting a microsphere with the diameter (D) about $150\mu m$, a corresponding tapered fiber with waist diameter $2.1\mu m$ is used to excite the microcavity WGMs evanescently. As shown in Fig. 4-b, the microsphere is fixed on the piezoelectric high-resolution translation stage (step resolution about 20 nm), to adjust the appropriate coupling position. Fig. 4-c shows a typical microcavity coupled with a taper. Fig. 4-d shows a typical resonant dip of the microsphere. It's important to note that experimental environment should be shockless to ensure the stable transmission spectra.
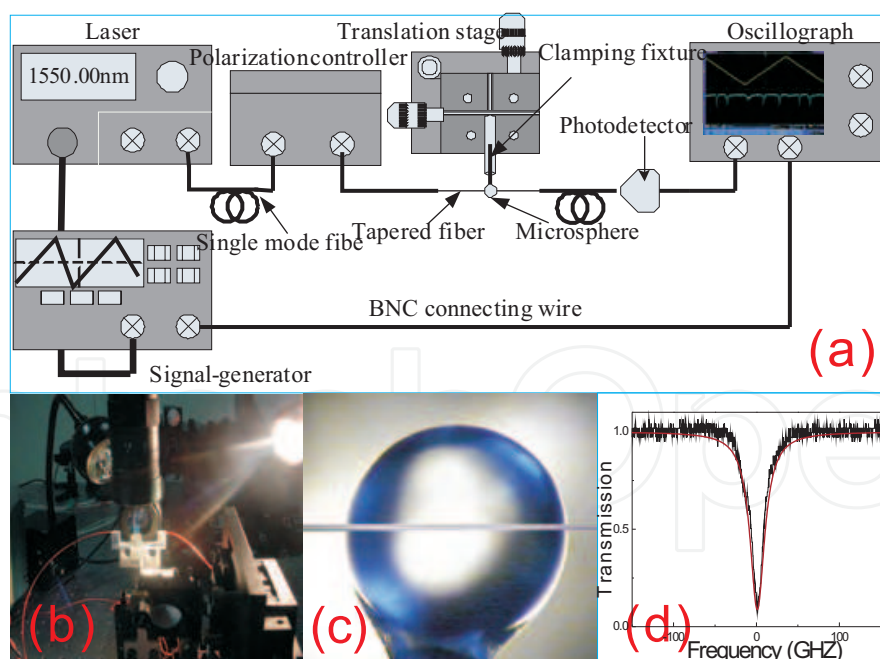

Fig. 4. (a) The schematic plan of the microsphere testing setup in our lab. (b) The experimental setting of the microsphere testing system in our lab. (c) A typical micrography of a microcavity coupled with a taper. (d) A typical resonant dip of the microsphere.

2.3 The challenging for practical application developments

Although there is great potential for the microcavity-based novel devices as illustrated in the "INTRODUCTION", there are some drawbacks of the traditional microsphere-taper system when promoting the above researches into practical applications.

First, the coupling efficiency can be affected, and the effective coupling can even be broken when loading the vibration on the taper or the microsphere, which challenges the robustness greatly. The robustness directly determines if the device is practical and can be used extensively. Thus, the robustness is the precondition for the microcavity-based practical devices.

Second, WGMs are very sensitive to the microcavity surroundings, which is an advantage for sensors, but makes the structure invalid in high RI materials or non-uniform dielectrics. For example, we can't measure the temperature of the Benzene, the Acetone or the Carbon disulfide disulphide et al, because the RI of these substances is higher than that of the silica which is frequently used to fabricate microcavities due to its low attenuation at the telecom band. The higher RI of the detected substance can destroy the resonance and subsequently fail the test. From this point of view, some special treatment are needed to improve this problem.

Third, the exposure of the traditional coupling system to the open environments makes the Q-maintenance challenging greatly, because the water and the dust in the air could spoil the Q drastically. The Q reduction can result in error signals to the functional devices. Therefore, realizing the Q maintenance is another aspect need to be solved.

Finally, high-resolution $3D$ translation stages are necessary in the traditional coupling system to adjust the coupling gap precisely. However, the stages are expensive and bulky, limiting the mobility in applications.

3. The solution to the problems

In this section, we propose one solution to the problems of the traditional microsphere-taper coupling system addressed above, and a package technology is proposed.

3.1 wholly-package manner

For the first time, we propose and realize a novel wholly packaged microsphere-taper coupling structure (PMTCS) experimentally (Y.-Z. Yan et al., 2011). The wholly-packaged structure is sketched by Fig. 5-a. We demonstrate that the PMTCS can avoid the problems addressed above, which is stable without $3D$ translation stages, robust against the vibration and free to move. Moreover, as a protective layer, the package body isolates the microsphere-taper from the surroundings, and maintains the Q above 10^6 for a long time.

To package the microsphere-taper coupling system, ultraviolet (UV) glue is used. The glue is fibre coating material with low RI ($n_g \approx 1.35$), which is made from special silicone acrylate with the product specification $KD - 310$. The packaging process is comprised of five steps, as shown in Fig. 5-b1 to b5. First of all, optimal coupling in the air with desirable resonant dips needs to be achieved, as shown in Fig. 5-b1. And then the UV glue is coated on the microsphere-taper by using a glue spreading machine in a dropping manner, as shown in Fig. 5-b2. Afterward, the package is solidify through 10 minutes exposure under a UV lamp, as shown in Fig. 5-b3. In the forth step, the microsphere stem, mounted on the 3D stages,
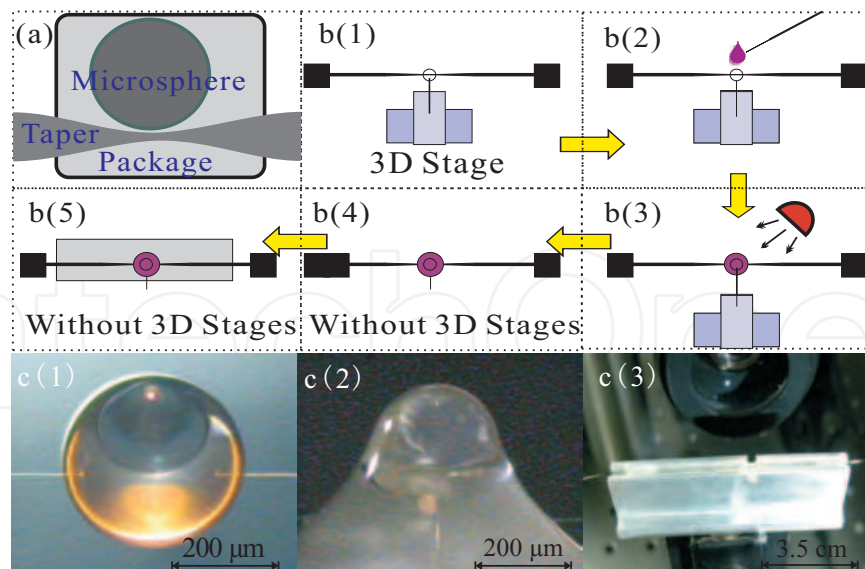
Fig. 5. (a) The schematic diagram of the wholly-packaged structure. b(1)-b(5) Illustration of the package process. c(1) The micrograph of the free microsphere coupling system after the forth step of the package. c(2) The micrograph of the semi-finished products of the packaged microcavity unit. c(3) A typical sealed packaged microsphere-taper coupling system.

is truncated by using a heat burning manner. The PMTCS here is independent of the $3D$ stages and can be moved freely, as shown in Fig. 5-a4 and Fig. 5-c1. Finally, similar to the potted circuit module we further package the structure using a designed slot as the mould to package the fragile taper totally (Fig. 5-b5). Fig. 5-c2 shows the semi-finished products of the wholly-packaged microcavity unit. Fig. 5-c3 shows a typical wholly-packaged module. In this module the microcavity, its coupling system and the fragile taper are all solidified into an entire body. The whole procedure is monitored by two microscopes, horizontally and vertically. It is worth noting that we need to re-adjust the coupling before the solidification, because the initial coupling is affected by the glue dropping which changes the environment and the surface tension around the microsphere as well as the taper. The resonant spectra fluctuate randomly at the first moment of the glue dropping, and gradually stabilize when the glue inosculates with the coupling structure after a few minutes. Particular attention has also to be paid to avoid the taper cracking, especially at its fragile taper waist.

Fig. 5-c1 shows a typical micrograph (side view) of a PMTCS ($D = 340\mu m$), in which the package body is asymmetric due to the gravity. As the backbone, the tapered fiber traverses across the package body to hold the PMTCS. At the package boundary (marked with blue triangles), there are two contact points which cause extra scattering loss (less than 20%). In the package experiments, the scattering loss can be reduced through using a shorter taper and encapsulating it completely, as shown in Fig. 5-c2 and Fig. 5-c3. This is also an effective way to improve the robustness which is determined by the un-stretched single-model fiber after packaging while depending on the fragile taper for an unpackaged system. In addition, the evanescent decay length (d) of WGMs ($d = \lambda/(2\pi\sqrt{n_s^2 - n^2})$, n_s and n are the RI of the microsphere and the surroundings, respectively.) increases from 0.1516λ to 0.3008λ, which causes a larger field overlap between WGMs and the taper. This makes the critical coupling easier to fulfill for a thicker taper. Besides, the coating layer with the minimum thickness

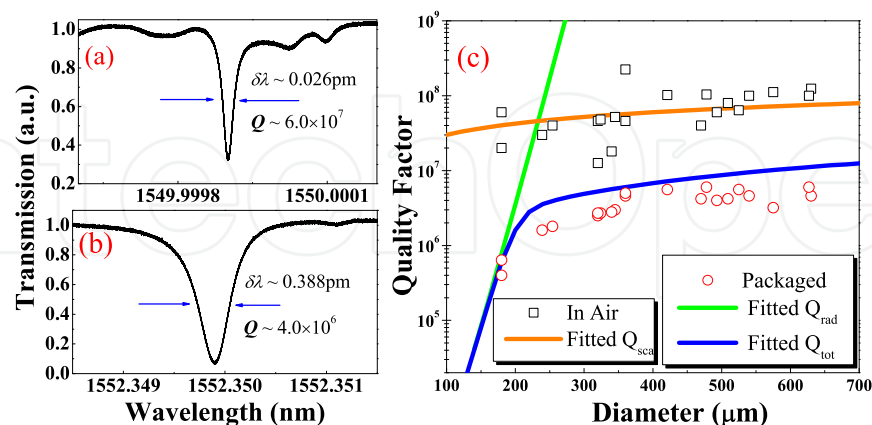about $2500\mu m$ ($\gg d$) ensures the complete isolation of WGMs from the outside, as shown in Fig. 5-c3.

Fig. 6. (a) and (b) are contrast resonant spectra for a microsphere ($D = 421\mu m$) before and after the packaging, respectively. (c) Tested and fitted Q versus microsphere D.

By comparing the spectra before and after the packaging, a red shift to the longer wavelength (S) has been observed, which can be estimated through $S = \frac{\lambda^2}{\pi D}(\frac{1}{\sqrt{n_s^2-n_g^2}} - \frac{1}{\sqrt{n_s^2-n_{air}^2}})$, where n_{air} is the air RI. For a microsphere with $D \approx 421\mu m$, the S we observed is $2.35nm$, which agrees well with theoretical prediction of $2.3nm$, as shown in Fig. 6-a and Fig. 6-b. The package can also eliminate high radial order WGMs and offer much more regular spectra. Because after the package, the relative RI (n_s/n) decreases from 1.44 to 1.07, corresponding to an increase of the total reflection critical angle from 43.62 to 70.92 degree, which results in much larger leakage for high radial order WGMs.

As the most important parameter of the microsphere, the intrinsic Q (Q_{tot}) of WGMs can be expressed as

$$Q_{tot}^{-1} = Q_{abs}^{-1} + Q_{sca}^{-1} + Q_{rad}^{-1}, \tag{1}$$

where Q_{abs}, Q_{sca} and Q_{rad} are related to the absorption, surface scattering and radiation loss, respectively (D. W. Vernooy et al., 1998). In our experiments, the microspheres are made of the commercial fiber, where high purity silica is used. This ensures Q_{abs} greater than 10^{10} in the air. Q_{sca} originates from the surface rayleigh scattering, and is mainly determined by the surface smoothness. For a microsphere induced by the surface-tension, the surface roughness is nanometer-sized ($1nm - 10nm$), which indicates the Q_{sca} above 10^8. The radiation loss of WGMs strongly depends on the size and RI of the cavity. At $1.55\mu m$ waveband, $Q_{rad} > 10^8$ can be achieved in the air for silica microspheres with D larger than $25\mu m$. In Fig. 6(c), we plot the measured Q_{tot} against D for the unpackaged microspheres by using white squares, where the recorded maximum Q_{tot} is around 10^8. Here, D is larger than $100\mu m$, indicating that the Q_{tot} is limited by the surface scattering loss, which agrees well with the fitted Q_{sca}.

However, compared with the unpackaged structure, Q_{tot} decreases apparently in the PMTCS. As shown by red circles in Fig. 6-c, the measured Q_{tot} decreases sharply when the diameter is less than $200\mu m$, and Q_{tot} is always smaller than 10^7 for larger microspheres. The similar phenomenon has been reported in microtoroids embedded in the water by Armani et al (A. M.

Armani, 2005). Former experiments have indicated that a coating on the microcavity surface can greatly reduce the Q_{sca}. Thus, the loss in the PMTCS mainly originates from the radiation loss and the glue absorption. We fit the Q_{tot} (blue line) with $n_g = 1.351 + 5 \times 10^{-6}i$ by analytically solving the WGMs in microsphere at $\lambda = 1550nm$. The results agree with the measurements greatly. Here, the imaginary part of n_g is corresponding to the amount of the absorption loss when the light propagates in the glue. With a real n_g=1.351, we obtain the Q_{rad} (green line) which decreases exponentially with the reduction in the diameter. In addition, particular attention should be paid to prevent contaminating the UV glue, because the contaminants attached to the microcavity or the taper can increase the overall scattering loss (M. L. Gorodetsky et al., 2000). On the contrary, mixing nano-particles at a certain concentration in the glue provides a feasible way to control the backscattering (X.-W. Wu et al., 2009). It is worth noting that the Q of the PMTCS is still much higher than the highest Q (2×10^5) of a packaged microfiber coil resonator (Y. Jung et al., 2010).
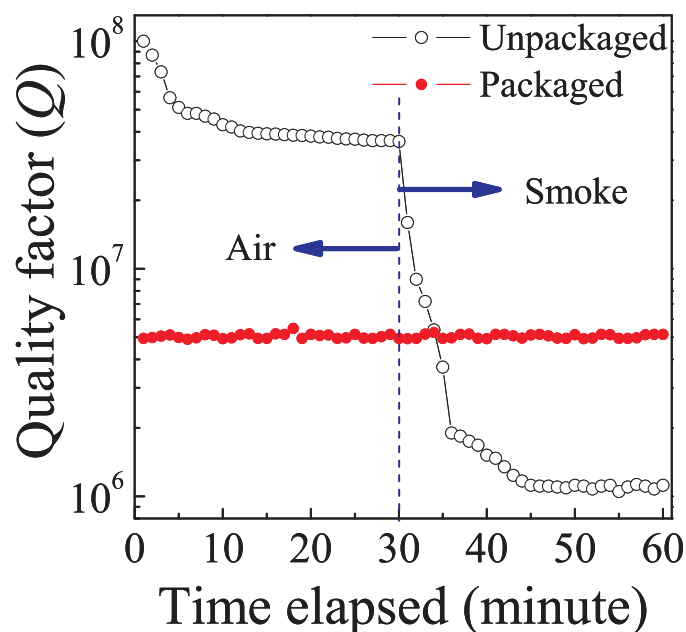

Fig. 7. Tested Q versus elapsed time of a microsphere coupling system in the air and in the smoke, for un-packaged (in black) and packaged (in red) samples, respectively.

It is obvious that the package body isolates the whole coupling system from the surroundings, excluding Q spoiling factors from the dust and water in the air. As shown in Fig. 7, when exposing a microsphere in the air, the Q shows a quick decay due to the water absorption in a few minutes after its fabrication. When putting it in the smoke, the Q has another remarkable decrease due to the scattering by the dust adhering to the surface. By contrast, the Q of PMTCS is much more stable and independent of the surrounding influences. In fact, we have maintained the Q above 10^6 for a few months. Thus, the package provides a feasible way to maintain the Q, paving the way for devices research in practical application.

3.2 Spot-package manner

WGMs of microspheres are attracting more and more attention recently due to their ultra-high quality factor (Q) values, very small volume and good compatibility with fiber-integrated optics, promising for a number of passive and active devices as filters, lasers and modulators. In the WGMs, light are well confined through total internal reflection (TIR) at the boundary,

and a small portion of energy exists outside the microsphere in the form of the evanescent field. The evanescent field is very important because it enables the WGMs to interact with the outside matters, such as atoms, nanoparticles, chemical and biological molecules. Thus, the WGMs are very potential for ultrasensitive sensors (J. T. Gohringa et al., 2010; J. Zhu et al., 2010; T. Lu et al., 2011).
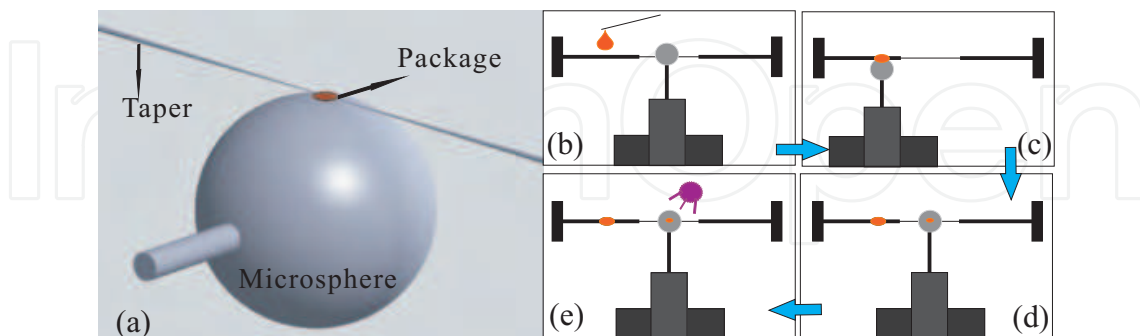

Fig. 8. (a) The schematic diagram of the spot-packaged microsphere-taper coupling system. (b)-(e) Illustration of the spot-package process. Red color represents the package glue.

In most applications, the fiber tapers are utilized to excite and collect the microsphere WGMs with high coupling efficiency. However, there are two principal drawbacks in the traditional microsphere-taper coupling system (MTCS) when exploring practical evanescent sensing devices. On one hand, in the external evanescent sensing applications the coupling region can be inserted or filled by the detected substance. The intrusion of the ectocrine in the coupling region can interfere in or destroy the microsphere-taper coupling, giving rise to fluctuations in the transmission spectra, and finally induce error signal for sensing. Therefore, the coupling region should be protected to avoid the insertion or filling of the detected substance. On the other hand, the MTCS lacks robustness, and a tiny vibration can change the relative positions of the taper and microsphere, subsequently influence the coupling efficiency and the resonant frequency. These instability limits the development of the practical sensors. Recently, we have realized a robust silica microsphere-taper coupling platform by using low refractive index (RI) curable polymer to encapsulate the coupling system wholly. This wholly-package enhances the robustness, isolates the coupling system from the surroundings, and makes the structure get rid of the burdensome fiber taper holders. These advantages are of immense importance for microcavity based gyro and temperature sensors. However, the wholly-package isolates the microsphere completely from external environments, preventing the interaction of the evanescent field with the matters outside.

In this part, we further improve the package technology for the MTCS. A novel spot-packaged structure is proposed and realized experimentally (Fig. 8-a). This structure not only holds the advantage of the robustness and stability, protects the coupling region, but also keeps the feasibility of the evanescent field sensing. This is potential for in-line optical sensors, and multiple microspheres can be integrated with the standard fiber, which can be applied to remote or distributed sensing applications in harsh environment.

The package process is comprised of four steps, as shown in Fig. 8-b to Fig. 8-e. First of all, after obtaining the optimal coupling in the air, the glue is dripped on one end of the un-stretched taper (Fig. 8-b). And then, by using two microscopes (horizontally and vertically, respectively) as the monitoring system, we adjust the microsphere to approach the glue attached to the fiber, as shown in Fig. 8-c. When an appropriate amount of the glue is

agglutinated on the microsphere, we adjust the microsphere away from the fiber. Afterward, we move the microsphere close to the taper again, as shown in Fig. 8-d. In this process, the coated spot-surface is controlled to contact with the taper gently. The coupling position is also modulated to achieve the fine resonant dips again. In the last step, the package is solidified through 10 minutes exposure under a UV lamp, as shown in Fig. 8-e. In addition, the stem of the microsphere can be burned out to release the microsphere from the $3D$ stages. Finally, we obtain the spot-packaged MTCS as shown in Fig. 8-a, which is integrated with fiber and can be moved freely and conveniently.
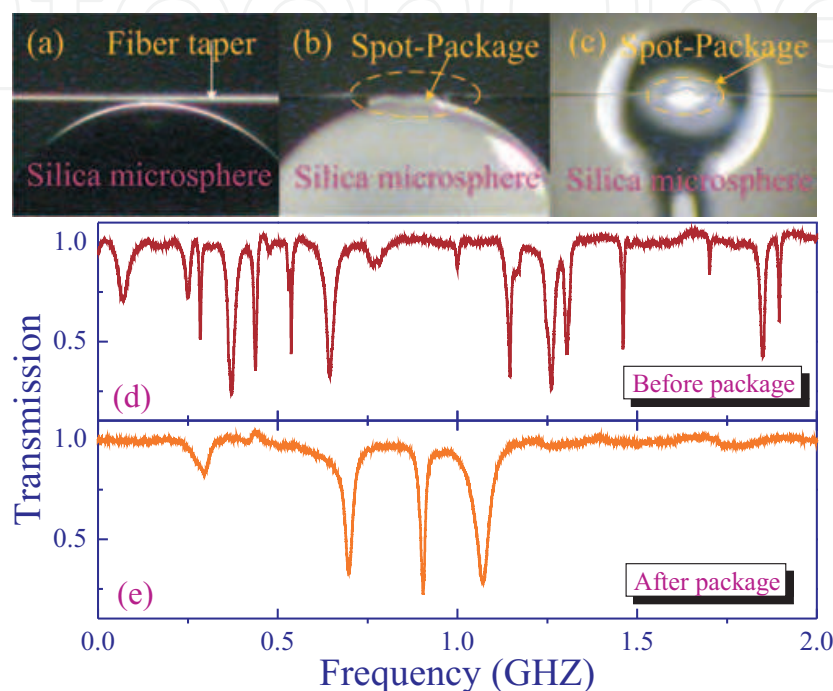

Fig. 9. (a) and (b) are the micrograph of a typical microsphere-taper coupling system before and after the spot-package process, respectively. (c) The side view of the spot-package. (d) and (e) are two typical transmission spectra of a microsphere before and after the spot-package process, respectively.

In Fig. 9-a and Fig. 9-b, we show typical micrographs of the MTCS without and with the spot-package. As shown clearly in Fig. 9-b, the coupling region surrounded by the glue is well protected from the external intrusion and vibration, while the rest of the silica microsphere surface are not affected. Therefore, the evanescent field can still interact with the matters near the microsphere. In addition, resulting from the liquid surface tension the glue surface is very smooth (similar to silica surface), which indicates that the package-induced scattering losses are almost negligible. Generally, the spot-package has an average area of about $30\mu m^2$, meaning that the spot-package occupies a circular arc length about $6\mu m$ at the equator of the silica microsphere (Fig. 9-c). As we will study below, the area of the package is the key factor to both the Q and the mechanic stability of the structure. Simply, the influence on WGMs is proportional to the rate $6/(\pi \times D)$ which describes the relative area of the package. From this perspective, microspheres with larger D are more suitable for this spot-package manner than the smaller ones.

Fig. 9-d and (e) are the transmission spectra before and after the spot-package, respectively. It is obvious that the resonant dips are broadened after the package, corresponding to a reduction of Q. It should be noted that this spot-packaged structure is essentially different from the wholly-packaged microsphere. In the wholly-packaged microsphere, light is confined at the silica-polymer interface. Since the boundary is rotational symmetric, the light ray undergoes continuous TIR at the boundary. The radiation loss and the polymer absorption are dominant, which respectively originates from the tunneling leak out at the low refraction contrast interface and the large polymer absorption. However, in the spot-packaged structure here (Fig. 9-b), the boundary of the spot-packaged microsphere is slightly deformed, which is a kind of asymmetric resonant cavities (ARC) (Y.-F. Xiao et al., 2009). In the ARC the properties are very different, because the rotational symmetric is broken. Thus, the light ray reflection at the boundary can't conserve the incident angle. Consequently, some rays refract out of the cavity after several reflection at the boundary. Hence, the Q is reduced after the spot-package process. Fig. 10-a, b and c show the numerical simulated electric field intensity of resonant modes in the spot-packaged microsphere. The critical total reflect angle at polymer/silica interface is $\chi_c = 68$ degree. Rays with large incidence angle $\chi > \chi_c$ can reflect at the silica boundary, so the incidence angle is well conserved. Therefore, for low radial order (high-Q) modes as shown in Fig. 10-a, the glue only gives small perturbations, and the energy is localized near the boundary, forming the modes as WGMs. For higher radial order (low-Q) modes as shown in Fig. 10-b and Fig. 10-c, rays reflect at the asymmetric boundary, resulting in chaotic ray dynamics and directional emission at the boundary. Therefore, only a few high-Q mode with large χ can survive in this ARC, leading to the much more regular spectra of the spot-packaged microsphere (Fig. 9-e).

To investigate the influence of the package on the Q, the Q before and after the spot-package was tested respectively by using the linewidth manner, in which the laser power was controlled to be lower than $5\mu W$ to avoid the thermal effect. Fig. 10(d) shows the measured highest Q for untreated and spot-packaged microspheres. It reveals that the Q for the spot-packaged microspheres are lower than that of the corresponding untreated sample. Although there is a decreasing of the loaded Q, the spot-packaged structure still has an average Q_{loa} about 1.02×10^7. With a tested average Q for the untreated microspheres about 4.2×10^7, the decreased factor has a average value about 4. The tested Q for the spot-packaged microsphere in our experiments is consistent with the former researches, which have demonstrated that high Q ($> 10^7$) WGMs can exist in a small deformation microsphere.

The spot-packaged structure also offers great mechanical stability, as the microresonator and the taper are integrated together via the solidified UV polymer. It provides feasibility for the microresonator to extricate itself from the bulky translation stages and makes the packaged structure be moved freely, which is of great significance for practical applications. By using a force measurement gauge, we tested the bearable loaded adhesive force for the packaged structure, as shown in Table I. The bearable loaded force grows with the increasing of the spot area. The force is about $50mN$ with the spot area about $30\mu m^2$ as mentioned above, which indicates that in such a regime a microsphere with the D of $300\mu m$ can endure an acceleration about $8.2 \times 10^4 g$. Actually, the robustness of this spot-packaged structure is limited by the strength of the fiber taper. As the maximum stress that a silica fiber taper can withstand is about $\delta_f \approx 10GPa$, a maximum force acting on the taper with the waist diameter $1\mu m$ is about $7.8mN$. Improvement of the stability of the spot-packaged regime by using a much more robust coupler, such as side-polished fiber and channel waveguide coupler, is undergoing.
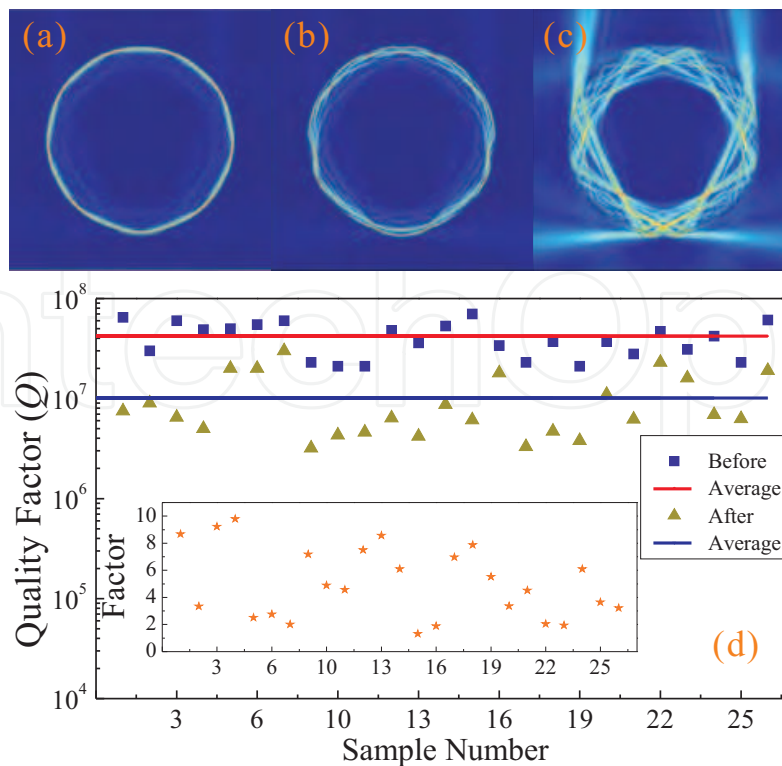
Fig. 10. (a), (b) and (c) The electric intensity distribution of three typical modes in the spot-packaged microsphere. (d) Tested Q of different microspheres before and after the spot-package. Insets: The decreased factor of the Q corresponds to different samples.

Spot Area (μm^2)	22 26 30 32 35 42 50 58 70
Force1 (mN)	35 39 51 54 58 59 65 72 82
Force2 (mN)	37 42 49 53 57 60 67 75 85
Force3 (mN)	32 46 53 55 60 61 69 74 87

Table 1. Force tested for different spot-package area

In this part, we have studied a novel spot-packaged MTCS by only encapsulating the coupling region with low RI polymer. The spot-package not only protects the coupling region, but also provides both mechanical and optical stability. In the packaged structure, Q greater than 10^7 is demonstrated with an average decreasing factor about 4 compared with the unpackaged microspheres. The Q decreasing is mainly due to the asymmetric boundary shape. The packaged MTCS can be integrated with fiber, and are expected to be used in practical external evanescent applications, including chemical and biological sensors. Especially, we believe that these in-line robust sensor can be used in harsh environments such as rockets, missiles and airborne crafts.

4. Practical sensing applications

To verify the practicability of the PTMCS, thermal sensing experiments are carried out in complex dynamic water environment. Generally, the temperature sensing is carried out by detecting the thermo-induced resonant wavelength shift. However, the shift can also be

induced by the changing of the microsphere surroundings, which is usually used to research the refractive index sensing. This phenomenon is the main obstacle for practical temperature sensors, because the refractive index of the open air is mutable. Here, in order to improve its sensing selectivity to only response to the temperature, the wholly-packaged microsphere is used as the sensing head. The package isolates the microsphere from the outside surroundings and eliminate the influence of the RI variation.

In sensing experiments, a beaker containing $600ml$ water with a stirrer in it is adopted as the testing environment, as shown in Fig. 11-a. The stirrer, not only helps to equalize the temperature, but also simulates a flowing water environment. A thermocouple and a heater are placed in the vicinity of the PMTCS, to measure and change the temperature, respectively.
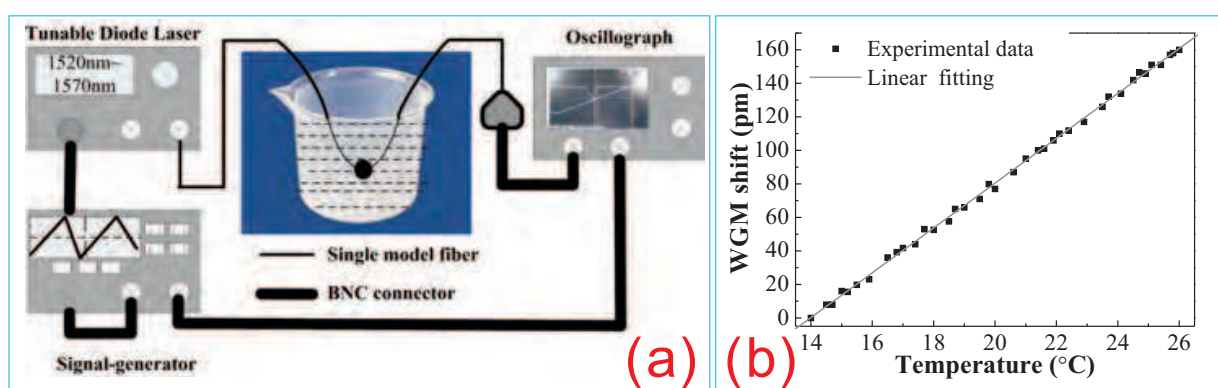

Fig. 11. (a) Temperature testing setup used in our expetiments. (b) WGM wavelength shifts as a function of the surrounding temperature, in NaCl resolution and in pure water, respectively.

The robustness is confirmed by the undisturbed spectra in the water flow. Furthermore, the completeness of the encapsulation is verified through the unshifted spectra when adding Sodium Chloride (NaCl) in the water gradually (keep the same temperature) to change the water RI about 2×10^{-3}, which could cause a WGM wavelength shift about $20pm$ for an unpackaged silica microsphere. Wavelength shifts against the temperature are recorded, in saturated NaCl solution and in pure water, respectively. As shown in Fig. 11-b, wavelength shifts are not affected by RI changes of the water. The temperature variation leads to changes both in the size and the RI of the silica microsphere, which subsequently causes resonance wavelength shifts (B.-B. Li et al., 2010; C.-H. Dong et al., 2009; Q. Ma et al, 2008; Y. Wu et al., 2009). The resonant wavelength shows a red shift about $160.39pm$ when the temperature increases from $14°C$ to $26°C$, which indicates a sensitivity of $13.37pm/°C$ with a relevant coefficient in linear fitting about 0.998. Taking into account the spectral resolution ($\Delta\lambda_{min}$) of our system, which is $0.015pm$, we estimate the resolution ($\Delta T_{min} = \Delta\lambda_{min}/(d\lambda/dT)$) of the PMTCS microsphere temperature sensor as $1.1 \times 10^{-3}°C$.

This resolution is in the same order of magnitude with the traditional silica microcavity thermal sensor. What's more, the practicability is greatly enhanced in the PMTCS, in which only the temperature change causes the WGM shift, while the change of external RI fails to cause the shift. Besides, the PMTCS thermal sensor shows an excellent anti-jamming ability, and can be used in harsh environments. Furthermore, the PMTCS can provide much more stable performance (for instance, the resolution) due to its superior Q maintenance ability.

Additionally, the bulky translation stages are no longer unnecessary in the PMTCS. The portable structure makes these sensors easy to move and miniature, which is important in practical applications, especially in microsystem technology research.

Further efforts will be focused on exploring new package materials and improving the package technology to enhance the packaged Q_{tot}. The PMTCS could be extended to multi-packaged microsphere-taper system on one fiber to monitor the real-time temperature at different locations, or package multi-microspheres in a certain point to study the classical analog to electromagnetic induced transparency (EIT) (Y.-F. Xiao et al, Y.-F. Xiao; J. Scheuer et al., 2006), even its application on gyroscopic (Y.-Z. Yan et al., 2011).

In addition, the wholly-packaged structure is also beneficial to the microcavity based filters, lasers et al. However, the wholly-package destroys the external evanescent field sensing which bases on the interaction of the WGMs with the detected substance. The spot-packaged structure can cover this shortage, making spot-packaged structure promising in RI, concentration or biochemical molecules.

In a word, when designing practical sensors we should choose an appropriate packaged structure (wholly-package or spot-package) according to the style of the sensing.

5. Conclusion

In summary, this chapter here proposed an novel package technology to solve the problems which hinders the improvements of microcavity based devices. Two package manners are realized, wholly-package and spot-package respectively. The fabrication and the tests of the two packages are illustrated in detail. The results show that, the packaged structures (wholly-package and spot-package) hold the striking merits to promote the developments of practical devices. In addition, the two manners are each with its own distinguishing features, and we should choose proper manner to use according to the devices we designed.

6. Acknowledgment

7. References

A. B. Matsko and V. S. Ilchenko. (2006). Optical Resonators With Whispering-Gallery Modes-Part I: Basics. *IEEE J. Quantum Electron*, Vol. 12, 3–14, ISSN: 0018-9197

A. Chiasera, Y. Dumeige, P. Fĺeron, M. Ferrari, Y. Jestin, G. Nunzi Conti, S. Pelli, S. Soria, and G.C. Righini. (2010). Spherical whispering-gallery-mode microresonators. *Laser Photonics Rev.*, Vol. 4, 457–482, ISSN: 1863-8880

A. M. Armani, D. K. Armani, B. Min, K. J. Vahala, and S. M. Spillane. (2005). Ultra-high-Q microcavity operation in H_2O and D_2O. *Appl. Phys. Lett.*, Vol. 87, 151118, ISSN: 0003-6951

B.-B. Li, Q.-Y. Wang, Y.-F. Xiao, X.-F. Jiang, Y. Li, L. Xiao, and Q. Gong. (2010). On chip, high-sensitivity thermal sensor based on high-Q polydimethylsiloxane-coated microresonator. *Appl. Phys. Lett.*, Vol. 96, 251109, ISSN: 0003-6951

C.-H. Dong, L. He, Y.-F. Xiao, V. R. Gaddam, S. K. Ozdemir, Z.-F. Han, G.-C. Guo, and L. Yang. (2009). Fabrication of high-Q polydimethylsiloxane optical microspheres for thermal sensing. *Appl. Phys. Lett.*, Vol. 94, 231119, ISSN: 0003-6951

C.-H. Dong, F.-W. Sun, C.-L. Zou, X.-F. Ren, G.-C. Guo, and Z.-F. Han. (2010). High-Q silica microsphere by poly(ethyl methacrylate) coating and modifying. *Appl. Phys. Lett.*, Vol. 96, 061106, ISSN: 0003-6951

D. W. Vernooy, V. S. Ilchenko, H. Mabuchi, E. W. Streed, and H. J. Kimble. (1998). High-Q measurements of fused-silica microspheres in the near infrared. *Opt. Lett.*, Vol. 23, 247–249, ISSN: 0146-9592

F. Vollmer, and S. Arnold. (2008). Whispering-gallery-mode biosensing: labelfree detection down to single molecules. *Nat. Methods*, Vol. 5, 591–596, ISSN: 1548-7091

F. Xu, and G. Brambilla. (2008). Demonstration of a refractometric sensor based on optical microfiber coil resonator. *Appl. Phys. Lett.*, Vol. 92, 101126, ISSN: 0003-6951

F. Xu, V. Pruneri, V. Finazzi, and G. Brambilla. (2008). An embedded optical nanowire loop resonator refractometric sensor. *Opt. Express*, Vol. 16, 1062–1067, ISSN: 1094-4087

I. M. White and X. Fan. (2008). On the performance quantification of resonant refractive index sensors. *Opt. Express*, Vol. 16, 1020–1028, ISSN: 1094-4087

J. C. Knight, G. Cheung, F. Jacques, and T. A. Birks. (1997). Phase-matched excitation of whispering-gallery-mode resonances by a fiber taper. *Opt. Lett.*, Vol. 22, 1129–1131, ISSN: 0146-9592

J. Scheuer, and A. Yariv. (2006). Sagnac Effect in Coupled-Resonator Slow-Light Waveguide Structures. *Phys. Rev. Lett.*, Vol. 96, 053901, ISSN: 0031-9007

J. T. Gohringa, P. S. Daleb, X. Fan. (2010). Detection of HER2 breast cancer biomarker using the opto-fluidic ring resonator biosensor. *Sens. Actuators, B*, Vol. 146, 226-230, ISSN: 0925-4005

J. Zhu, S. K. Ozdemir, Y. F. Xiao, L. Li, L. He, D. R Chen, L. Yang. (2010). On-chip single nanoparticle detection and sizing by mode splitting in an ultrahigh-Q microresonator. *Nat. Photonics*, Vol. 4, 46-49, ISSN: 1749-4885

K. J. Vahala. (2003). Optical microcavities. *Nature*, Vol. 424, 839–846, ISSN: 0028-0836

M. L. Gorodetsky, A. A. Savchenkov, and V. S. Ilchenko. (1996). Ultimate Q of optical microsphere resonators. *Opt. Lett.*, Vol. 21, 453–455, ISSN: 0146-9592

M. Cai, O. Painter, and K. J. Vahala. (2000). Observation of Critical Coupling in a Fiber Taper to a Silica-Microsphere Whispering-Gallery Mode System. *Phys. Rev. Lett.*, Vol. 85, 74–77, ISSN: 0031-9007

M. L. Gorodetsky, A. D. Pryamikov, and V. S. Ilchenko. (2000). Rayleigh scattering in high-Q microspheres. *J. Opt. Soc. Am. B*, Vol. 17, 1051–1057, ISSN: 0740-3224

M. Hossein-Zadeh, and K. J. Vahala. (2006). Fiber-taper coupling to Whispering-Gallery modes of fluidic resonators embedded in a liquid medium. *Opt. Express*, Vol. 14, 10800–10810, ISSN: 1094-4087

M. Sumetsky, R. S. Windeler, Y. Dulashko and X. Fan. (2007). Optical liquid ring resonator sensor. *Opt. Express*, Vol. 15, 14376-14381, ISSN: 1094-4087

Q. Ma, T. Rossmann and Z. Guo. (2008). Temperature sensitivity of silica micro-resonators. *J. Phys. D: Appl. Phys.*, Vol. 41, 245111, ISSN: 0022-3727

X.-W. Wu, C.-L. Zou, J. M. Cui, Y. Yang, Z.-F. Han and G. C. Guo. (2009). Modal coupling strength in a fibre taper coupled silica microsphere. *J. Phys. B: At. Mol. Opt. Phys.*, Vol. 42, 085401, ISSN: 0953-4075

Y. Sun, and X. Fan. (2008). Analysis of ring resonators for chemical vapor sensor development. *Opt. Express*, Vol. 16, 10254–10268, ISSN: 1094-4087

Y. Jung, G. S. Murugan, G. Brambilla, and D. J. Richardson. (2010). Embedded optical microfiber coil resonator with enhanced high-Q. *Photon. Technol. Lett.*, Vol. 22, 1638–1640, ISSN: 1041-1135

Y. Wu, Y.-J. Rao, Y.-H. Chen and Y. Gong. (2009). Miniature fiber-optic temperature sensors based on silica/polymer microfiber knot resonators. *Opt. Express*, Vol. 17, 18142–18147, ISSN: 1094-4087

Y.-F. Xiao, X.-B. Zou, W. Jiang, Y.-L. Chen, and G.-C. Guo. (2007). Analog to multiple electromagnetically induced transparency in all-optical drop-filter systems. *Phys. Rev. A*, Vol. 75, 063833, ISSN: 1050-2947

Y.-F. Xiao, C.-H. Dong, C.-L. Zou, Z.-F. Han, L. Yang, and G.-C. Guo. (2009).Low-threshold microlaser in a high-Q asymmetrical microcavity. *Opt. Lett.*, Vol. 34, 509-511, ISSN: 0146-9592

Y.-Z. Yan, C.-L. Zou, S.-B. Yan, F.-W. Sun, Z. Ji, J. Liu, Y.-G. Zhang, L. Wang, C.-Y. Xue, W.-D. Zhang, Z.-F. Han, and J.-J. Xiong. (2011). Packaged silica microsphere-taper coupling system for robust thermal sensing application. *Opt. Express*, Vol. 19, 5753-5759, ISSN: 1094-4087

Y.-Z. Yan, Z. Ji, S.-B. Yan, J. Liu, C.-Y. Xue, W.-D. Zhang, J.-J. Xiong. (2011). Enhancing the Robustness of the Microcavity Coupling System. *Chin. Phys. Lett*, Vol. 28, 034208, ISSN: 0256-307X

Fiber Optic Sensors

Edited by Dr Moh. Yasin

This book presents a comprehensive account of recent advances and researches in fiber optic sensor technology. It consists of 21 chapters encompassing the recent progress in the subject, basic principles of various sensor types, their applications in structural health monitoring and the measurement of various physical, chemical and biological parameters. It also highlights the development of fiber optic sensors, their applications by providing various new methods for sensing and systems, and describing recent developments in fiber Bragg grating, tapered optical fiber, polymer optical fiber, long period fiber grating, reflectometry and interefometry based sensors. Edited by three scientists with a wide knowledge of the field and the community, the book brings together leading academics and practitioners in a comprehensive and incisive treatment of the subject. This is an essential reference for researchers working and teaching in optical fiber sensor technology, and for industrial users who need to be aware of current developments and new areas in optical fiber sensor devices.

How to reference

In order to correctly reference this scholarly work, feel free to copy and paste the following:

Ying-Zhan Yan, Shu-Bin Yan, Zhe Ji, Da-Gong Jia, Chen-Yang Xue, Jun Liu, Wen-Dong Zhang and Ji-Jun Xiong (2012). Robust Fiber-Integrated High-Q Microsphere for Practical Sensing Applications, Fiber Optic Sensors, Dr Moh. Yasin (Ed.), ISBN: 978-953-307-922-6, InTech, Available from: http://www.intechopen.com/books/fiber-optic-sensors/robust-fiber-integrated-high-q-microsphere-for-practical-sensing-applications

INTECH
open science | open minds